Asian Journal of Chemistry; Vol. 35, No. 2 (2023), 522-528

ASIAN JOURNAL OF CHEMISTRY

https://doi.org/10.14233/ajchem.2023.27004

Theoretical Study of D-π-A Structured Malvidin for DSSC Application

X. MARY JOSEPHINE[1], R. RAJMUHAMED[1], S. KRISHNAVENI[2] and V. SATHYANARAYANAMOORTHI[2,*]

[1]Department of Physics, Jamal Mohamed College (Autonomous), (Affiliated to Bharathidasan University), Tiruchirappali-620020, India
[2]Department of Physics, PSG College of Arts and Science (Autonomous), Coimbatore-641014, India

*Corresponding author: E-mail: sathyanarayanamoorthi@yahoo.co.in

Received: 8 December 2022; *Accepted*: 25 January 2023; *Published online*: 30 January 2023; AJC-21139

Six novel dye molecules were developed from D-π-A system and their suitability for dye sensitized solar cells (DSSCs) was evaluated using density functional theory (DFT). All the calculation were performed using B3LYP/6-311++ G (d,p) level basis set. The intermolecular charge transfer was examined using Frontier molecular orbitals. The absorption spectra, light harvesting efficiency (LHE) and the electron injection energy (ΔG_{inject}) for all the designed dyes were calculated to compare their photovoltaic performance. All of these dyes developed in this study show great potential as a DSSC sensitizer.

Keywords: Dye sensitized solar cells, Malvidin, Light harvesting efficiency, Natural dyes.

INTRODUCTION

Due to its low production cost, the dye-sensitized solar cell (DSSC) is being studied as a potential future alternative energy source [1,2]. The DSSC can convert light energy to an electrical energy [3,4]. The photosensitization effect of the dye pigment influences the light absorption spectrum [5,6]. Due to their numerous benefits, such as low cost, a wide range of specific functional groups, a high molar extinction coefficient, an easy technique of extraction and environmental friendliness, natural dyes are rapidly gaining appeal as an alternative to noble metal complexes. There is a push-pull structure (D-π-A) in natural dye sensitizers, where an electron donor (D) is linked to an electron acceptor (A) *via* π-conjugated system [7-9]. The photovoltaic efficiency of DSSC is affected by the structure of the organic dye used. By switching up the electron donor group, π-conjugated system, or acceptor group, D-π-A dyes can take on a wide range of optical and electronic properties.

In this theoretical study, a new organic dye-sensitized solar cell (DSSCs) having a D-π-A structure with a triphenylamine (TPA) and diphenylamine (DPA) moiety as an electron donor (D) and cyano and nitro as an electron acceptor (A) and malvidin as a π-conjugated system is designed, which are shown in Fig. 1. By altering the molecular structure of malvidin, new dyes were designed. The structure of malvidin and newly designed dyes are shown in Fig. 2 and 2a. Malvidinis the basic structure of the anthocyanidin. The anthocyanidins (also known as aglycons) are composed of three separate aromatic rings bonded together through carbon-carbon bonds. One of these aromatic

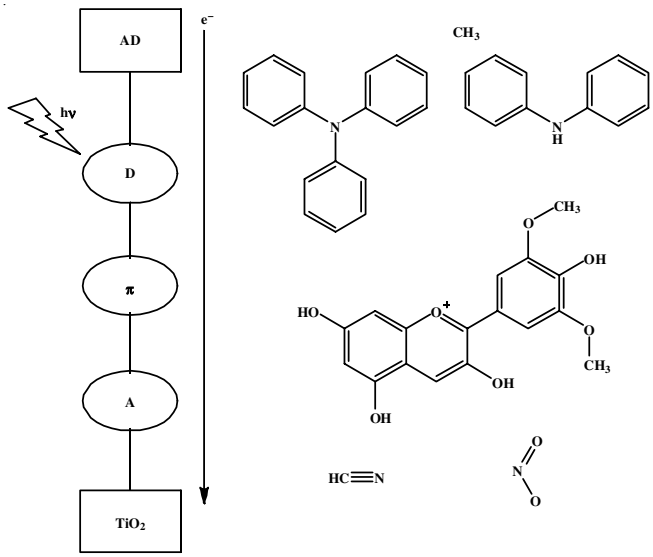

Fig. 1. Different parts of AD-D-π-A system. AD = auxiliary donor, D = donor, π = pi-spacer, A = acceptor

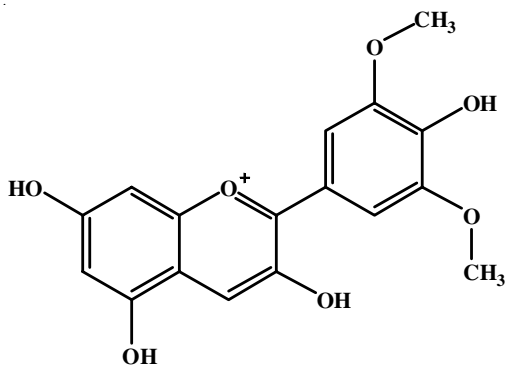

Fig. 2. Chemical structure of malvidin

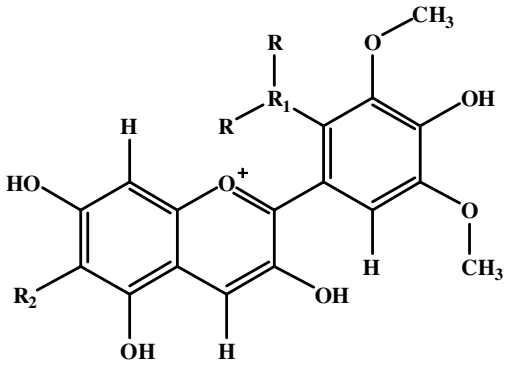

Ma1: $R_1 = C_{12}H_{10}N$; $R_2 = CN$
Ma2: $R_1 = C_{18}H_{14}N$; $R_2 = NO_2$
Ma3: $R_1 = C_{12}H_{10}N$; $R_2 = CN$
Ma4: $R_1 = C_{18}H_{14}N$; $R_2 = NO_2$
Ma5: $R_1 = C_{18}H_{14}N$; $R_2 = CN$; $R = CH_3$
Ma6: $R_1 = C_{18}H_{14}N$; $R_2 = NO_2$; $R = CH_3$

Fig. 2a. Chemical structure of newly designed dyes

rings is linked to an oxygen-containing heterocyclic ring [10]. Malvidin is abundantly present in all grape varieties and can be considered as the main component, which is responsible for the colour of red grapes and red wine [11]. The most effective strategy to get around difficulties in experimental synthesis and investigating the possibilities that reduce the material manufacture and processing cost is to utilize theoretical techniques. DFT is a viable solution for these challenges since it investigates the electronic structure and spectroscopic characteristics. In this work, the electronic structure, absorption spectra and photovoltaic properties were calculated by using DFT and TD-DFT methods [12].

COMPUTATIONAL METHODS

The density functional theory with B3LYP/6-311++G(d,p) basis set was used for all calculation in gas and solvent phase [13,14]. The excited state energies, electron absorption spectra and oscillator strengths (f) were investigated by employing CAM-B3LYP/6-311++G(d,p) basis set. In DFT calculations, the lowest-lying excitation energy is best estimated by considering in the long-range correction. Hence, the CAM-B3LYP is the method of choice for simulation of absorption spectrum [15]. All calculations in the solvent phase adopted the polarizable continuum model (PCM) [16]. The solvents used for these calculations were dimethylformamide (DMF) and dichloromethane (DCM). All computations were performed in Gaussian 09 and GaussView Version 5.0 was used to display the models of electron density at various energy levels [17].

RESULTS AND DISCUSSION

Frontier molecular orbitals: To determine whether the suggested dyes satisfy the DSSC photosensitizer criteria, the highest occupied molecular orbital (HOMO) and lowest unoccupied molecular orbital (LUMO) for each dye could be computed at the B3LYP/6-311++G(d,p) level of theory [18]. The intramolecular charge transfer (ICT) behaviour in the DSSC devices can be understood from the structures of HOMO and LUMO. The HOMO, LUMO and energy gaps of the designed dyes are reported in Table-1, while the distribution patterns of HOMO and LUMO of malvidin and newly designed sensitizer, Ma1-Ma6 are depicted in Fig. 3 for gas phase.

In malvidin, the HOMO is delocalized over the entire molecule. The LUMO of malvidin is dispersed throughout the molecule. The HOMOs are localized on the donor part, for designed dyes Ma4-Ma6 whereas for dyes Ma1-Ma3, the HOMOs are localized on part of donor and π-spacer. The electron density of the LUMO is mainly localized on the electron acceptor fragment with delocalization onto the π-linker for all designed dyes. It is desirable to have such electron density distribution for effective electron injection and charge separation.If the dyes are effective sensitizers as anticipated, it is because of the charge transfer from donor to acceptor through the π-spacer. Spontaneous charge transfer from the dye excited state to conduction band of TiO_2 require more positive LUMO energy than $E_{cb}^{TiO_2}$ (-4.0 eV), while the spontaneous charge regeneration needs more negative HOMO energy than the

TABLE-1
E_{HOMO}, E_{LUMO} AND ENERGY GAP (E_g) OF DYES IN eV AT B3LYP/6-311++G (d,p) LEVEL OF THEORY

Dye	Gas phase			DMF			DCM		
	HOMO	LUMO	E_{gap}	HOMO	LUMO	E_{gap}	HOMO	LUMO	E_{gap}
Malvidin	-9.2059	-6.5720	2.6335	-6.4837	-3.5728	2.9108	-6.7204	-3.8463	2.8740
Ma1	-7.5136	-6.6227	0.8909	-4.7884	-3.8833	0.9050	-5.0439	-4.1418	0.9020
Ma2	-7.6189	-6.7092	0.9096	-4.8651	-3.9478	0.9175	-5.1255	-4.2085	0.9170
Ma3	-7.4676	-6.5977	0.8699	-4.8651	-3.9775	0.8876	-5.1160	-4.2308	0.8851
Ma 4	-7.6350	-6.5062	1.1287	-4.9639	-3.8218	1.1420	-5.2224	-4.0822	1.6705
Ma 5	-7.5074	-6.3735	1.1339	-4.9587	-3.8142	1.1445	-5.2023	-4.0599	1.1423
Ma 6	-7.5332	-6.3979	1.1352	-5.2268	-4.0852	1.1415	-5.2268	-4.0852	1.1415

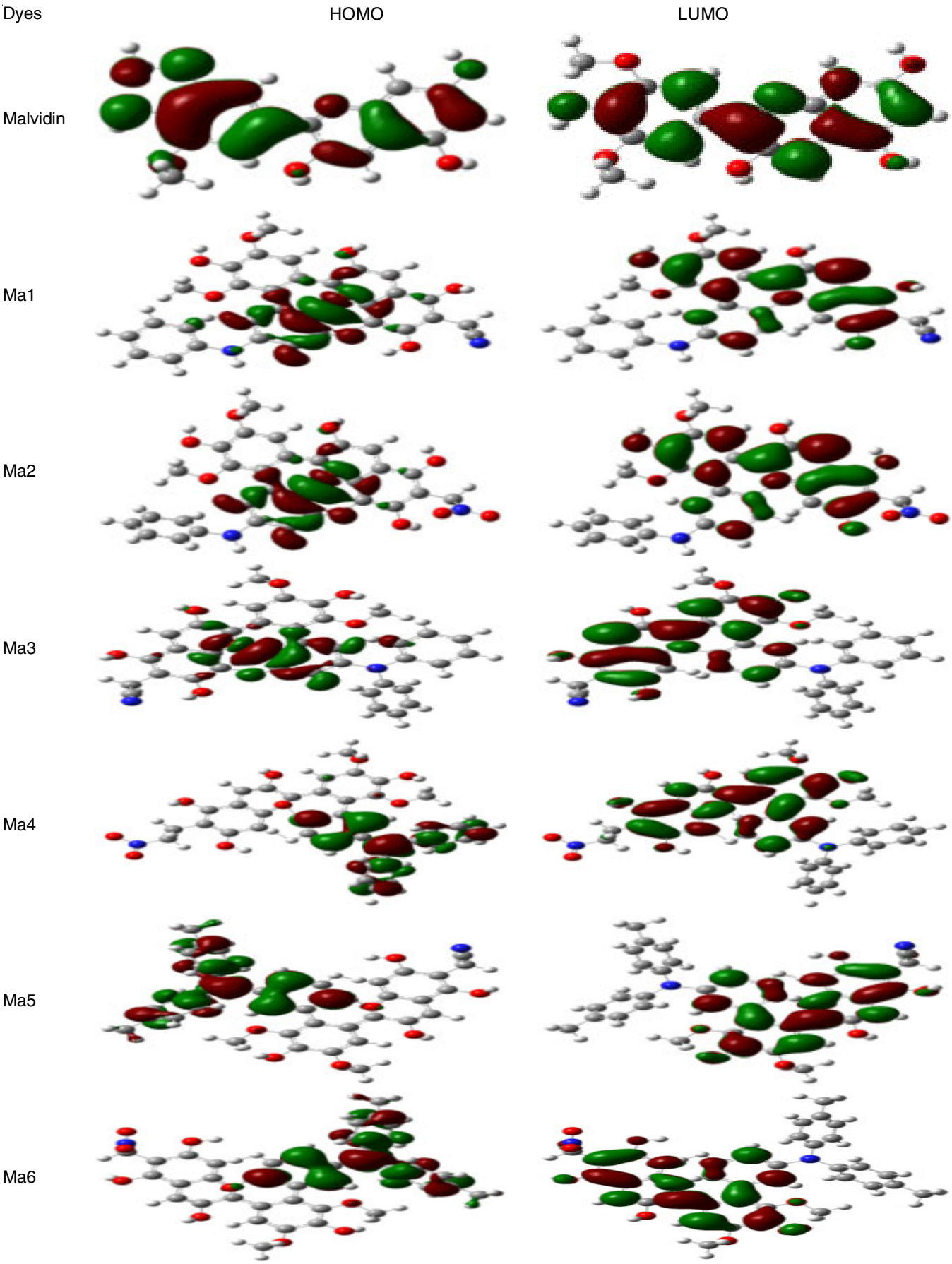

Fig. 3. HOMO and LUMO distribution pattern of malvidin based dyes at DFT/B3LYP/6-311++G (d,p) level of theory in gas phase

reduction potential energy of the I^-/I^{3-} electrolyte (-4.8 eV). Each of the newly developed dyes has a LUMO which is higher than the conduction band energy (E_{cb}) of TiO_2, while each of their HOMOs is lower than the redox potential energy of the electrolyte in DMF solvent phase.

HOMO-LUMO energy gap: The metal-free organic dyes depend their functionality to intramolecular charge transfer (ICT) between the donor and anchoring group *via* the π-spacer. This feature is influenced by the molecule's energy gap, which also influences the photocurrent [13]. The smaller the energy gap, the easier it is to move electrons from HOMO to LUMO levels by absorption of light energy of the appropriate wavelength [19]. The HOMO and LUMO energy gap of the dyes in gas and solvent phases are shown in Table-1. In comparison to the other dye derivatives, the Ma3 dye has the smallest energy gap. This indicates that an electron can readily to be transferred from HOMO to LUMO. As a result, when compared to other dye molecules investigated, Ma3 dye appears to be a viable candidate for use in DSSC. Short-circuit current density and power conversion efficiency in DSSCs are improved when the HOMO-LUMO energy gap is small, as more photons are absorbed and excited into the LUMO molecular orbitals. The calculated energy gapvalues range from about 0.8699 eV to 1.1415 eV, denoting that all these dyes Ma1-Ma6, has the potential to be used in DSSCs.

Effect of solvent on HOMO-LUMO energies: By using the solvation effect in DFT calculations of HOMO and LUMO, the differences between experiment and computational are minimized. According to Ekanayake *et al.* [20], there are no major shifts in the band gap when the solvation effect is calculated, although the absolute values of the HOMO and LUMO do shift. This suggests that the band gap is unaffected by vacuum and hence the computations result in an over-estimation of the energy level. Similar performance was seen between malvidin and the newly developed dyes in this study. Solvents have a higher HOMO energy than gases do. Its LUMO energy is less in the gas phase than it is in the solvent phase. Furthermore, DMF and DCM are aportic polar solvents; they raise the value of HOMO and LUMO energy. The calculated energy gap in the solvent phase is lower than in the gas phase as a result of these effects. The energy level diagram of HOMO, LUMO, conduction band energy of (E_{cb}) of TiO_2 and redox potential energy of the electrolyte in gas and solvent phase are shown in Figs. 4-6.

Free energy change of electron injection and oxidation potential: Both the excited state oxidation potential of the dye and the free energy shift for electron injection onto a titanium dioxide (TiO_2) surface were calculated using the the following mathematical equations. The following equation was used to calculate the free energy change for the process of electron injection [21]:

$$\Delta G^{inject} = E_{ox}^{dye*} - E_{CB}^{TiO_2} \quad (1)$$

where E_{ox}^{dye*} is the excited state oxidation potential of the dye and $E_{CB}^{TiO_2}$ is the energy of conduction band of TiO_2 semiconductor (–4.0 eV). The E_{ox}^{dye*} can be determined by the following equation [21]:

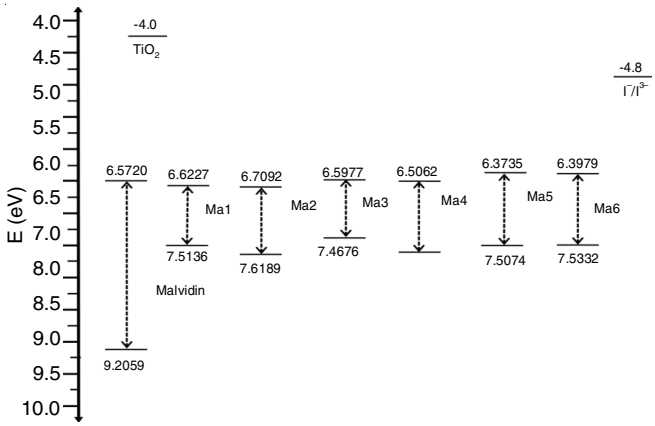

Fig. 4. Schematic energy diagram (E_{HOMO} and E_{LUMO}) of the dyes in gas phase

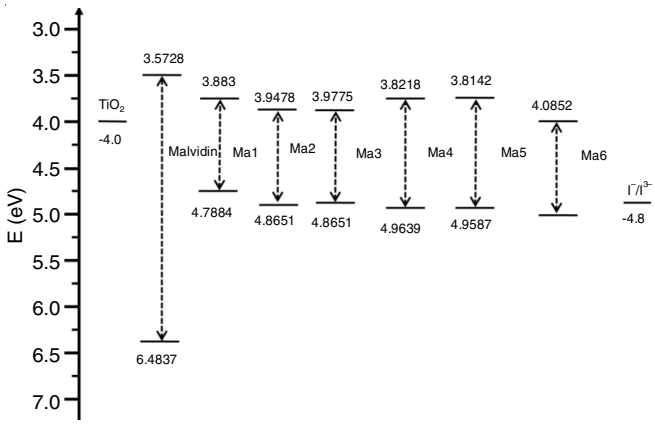

Fig. 5. Schematic energy diagram (E_{HOMO} and E_{LUMO}) of the dyes in DMF

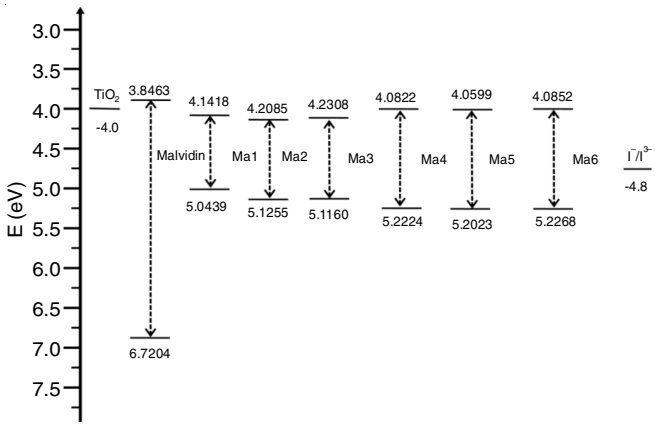

Fig. 6. Schematic energy diagram (E_{HOMO} and E_{LUMO}) of the dyes in DCM

$$E_{ox}^{dye*} = E_{ox}^{dye} - \lambda_{max}^{ICT} \quad (2)$$

where E_{ox}^{dye} is the oxidation potential energy of dye in ground state ($E_{ox}^{dye} = -E_{HOMO}$) and λ_{max}^{ICT} is the vertical transition energy corresponding to λ_{max}. The ground state (E_{ox}^{dye}) and excited state oxidation potential (E_{ox}^{dye*}) and the electron injection free energy change (ΔG^{inject}) are computed in gas phase as well as in solvent phase are presented in Table-2. The ΔG^{inject} values are negative for all newly designed dyes. In malvidin and newly designed dyes ΔG^{inject} value in gas phase showed endergonic type electron injection. The value of ΔG^{inject} ismore negative than malvidin for all newly designed dyes in solvent phase. In all designed

TABLE-2
CALCULATED ABSORPTION MAXIMA (λ_{max}), INTRAMOLECULAR CHARGE TRANSFER ENERGY (λ_{max}^{ICT}) , OXIDATION POTENTIAL (E_{OX}^{dye*}) , ELECTRON INJECTION ENERGY (ΔG^{inject}) OF MALVIDIN BASED DYES AT B3LYP/6-311++G (d,p) LEVEL OF THEORY

Dye	Gas phase				DMF				DCM			
	λ_{max}	λ_{max}^{ICT}	E_{OX}^{dye*}	ΔG^{inject}	λ_{max}	λ_{max}^{ICT}	E_{OX}^{dye*}	ΔG^{inject}	λ_{max}	λ_{max}^{ICT}	E_{OX}^{dye*}	ΔG^{inject}
Malvidin	546.15	2.2702	6.9357	2.9357	489.63	2.5322	3.9515	-0.0485	497.22	2.4936	4.2268	0.2268
Ma1	734.60	1.688	5.8258	1.8258	639.87	1.9376	2.8508	-1.1492	656.47	1.8887	3.1552	-0.8448
Ma2	742.72	1.6693	5.9496	1.9496	693.69	1.7873	3.0778	-0.9222	713.17	1.7385	3.387	-0.613
Ma3	779.79	1.5941	5.8735	1.8735	664.7	1.8653	2.9998	-1.0002	683.03	1.8152	3.3008	-0.6992
Ma4	795.40	1.7187	5.9163	1.9163	735.16	1.6865	3.2774	-0.7226	756.80	1.6383	3.5841	-0.4159
Ma5	721.84	1.7176	5.7898	1.7898	660.29	1.8777	3.0810	-0.9190	670.64	1.8488	3.3535	-0.6465
Ma6	725.36	1.7093	5.8239	1.8239	694.56	1.7851	3.4417	-0.5583	676.28	1.8333	3.0785	-0.9215

dyes *viz*. Ma1, Ma2, Ma3, Ma4, Ma5 and Ma6, the ΔG^{inject} was improved in gas phase as well as in solvent phase (Table-2). The ΔG^{inject} is negative for all studied dyes in solvent phase. Since the excited state of the dye would be above the edge of the conduction band in TiO_2, this reveals the spontaneous nature of the electron injection process [18].

Absorption properties: The UV/visible absorption spectra of all the sensitizers simulated in gas and solvent phase at the TD-DFT/CAM-B3LYP/6-311++G(d,p) level are shown in Fig. 7. The computed maximum absorption wavelength (λ_{max}), absorption energy, oscillator strengths (f) are summarized in Table-3. It is demonstrated that all the six designed dyes Ma1–Ma6 exhibited strong absorption in the visible spectrum. Absorbance in visible region is required for high efficiency of DSSCs. The presence of electron donor benefits the red shift. As for Ma1-Ma6, the maxima of absorption peaks for all the designed molecules have a red-shift when compared with the reference molecule malvidin (546.15 nm). For newly designed sensitizers Ma1-Ma6, extraordinary red shifts can be seen in the absorption spectra at 734.60 nm, 742.74 nm, 779.79 nm,

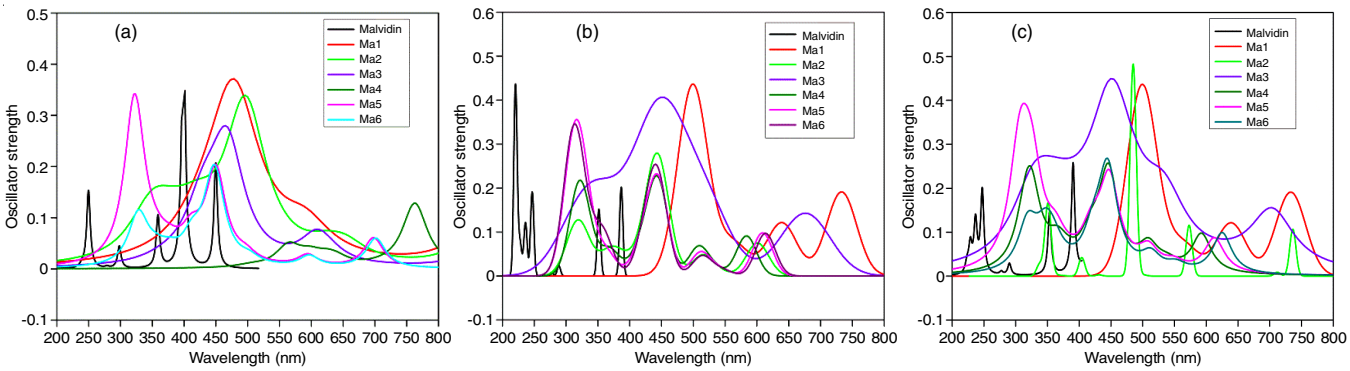

Fig. 7. Stimulated UV-visible absorption spectra of dyes calculated in (a) gas phase (b) DMF (c) DCM at CAM-B3LYP/6-311++ G(d,p) level of theory

TABLE-3
MAXIMUM ABSORPTION WAVELENGTH (λ_{max}), LIGHT HARVESTING EFFICIENCY (LHE), AVERAGE LIGHT HARVESTING EFFICIENCY (LHE_{avg}), OSCILLATOR STRENGTH (f) OF MALVIDIN BASED DYES AT CAM-B3LYP/6-311++ G(d,p) LEVEL OF THEORY

Dye	Gas phase				DMF				DCM			
	λ_{max}	f	LHF	LHE_{avg}	λ_{max}	f	LHF	LHE_{avg}	λ_{max}	f	LHF	LHE_{avg}
Malvidin	449.74	0.2049	0.3761	0.2922	386.75	0.2019	0.3717	0.3344	390.34	0.2502	0.4379	0.3580
	358.91	0.1015	0.2084		351.62	0.1519	0.2951		353.34	0.1424	0.2778	
Ma1	590.82	0.0602	0.1294	0.3336	508.95	0.2908	0.4880	0.5065	521.51	0.2284	0.4089	0.4942
	478.32	0.3352	0.5378		453.64	0.3234	0.5251		461.00	0.3763	0.5795	
Ma2	496.61	0.3106	0.5108	0.3348	600.89	0.0749	0.1584	0.2880	484.98	0.4828	0.6709	0.4939
	353.67	0.0752	0.1589		443.87	0.2348	04176		350.90	0.1656	0.3170	
Ma3	629.36	0.6089	0.7539	0.4665	518.10	0.1553	0.3006	0.4192	703.47	0.1329	0.2636	0.3772
	428.84	0.0858	0.1792		447.03	0.3352	0.5378		452.96	0.2932	0.4909	
Ma4	762.81	0.1265	0.2527	0.2390	583.63	0.0911	0.1892	0.2808	446.38	0.2157	0.3914	0.3404
	564.11	0.0406	0.0892		447.78	0.2008	0.3702		323.88	0.1484	0.2894	
Ma5	450.00	0.1778	0.3359	0.3840	445.02	0.2082	0.3808	0.3566	447.48	0.2001	0.3691	0.3412
	321.07	0.2458	0.4321		324.74	0.1756	0.3325		305.35	0.1632	0.3132	
Ma6	449.14	0.1503	0.2925	0.2319	441.81	0.1568	0.3017	0.2858	443.54	0.1292	0.2573	0.2324
	328.12	0.0817	0.1714		309.93	0.1367	0.2700		318.68	0.1011	0.2076	

*Oscillator strength > 0.1 are shown

721.40 nm, 721.84 nm and 725.36 nm in the gas phase. It is expected that designed Ma1-Ma6 dyes will be able to produce more light at the longer wavelength, which is beneficial for further increasing the photo-to-electric conversion efficiency of the corresponding solar cells due to the absorption shift to greater wavelengths favouring the illumination process. The absorption peaks has shown hypsochromic shift in the solvent phase as compared to gas phase. The decrease in absorption wavelength (UV-Vis) in thesolvent phase (Fig. 7) is due to the addition of polar solvent [13,14]. As a result, it is concluded that introducing electron donor and acceptor units to improve the absorption spectra is a validating step.

Light harvesting efficiency (LHE): The light harvesting efficiency (LHE) measures the dye's ability to respond to light. To maximize the photocurrent response, the LHE of the dye sensitizer should be as high as feasible, as calculated by the following equation [22]:

$$LHE = 1 - 10^{-f} \quad (3)$$

where 'f' is the oscillator strength of dye and is the wavelength where the peak absorbance is achieved through intramolecular charge transfer. The oscillator strength is directly obtained from TD-DFT calculations. The maximum oscillator strength (f) and LHE for malvidin and newly designed dyes are reported in Table-3. Only the transitions with considerable oscillator strengths are shown. All newly designed dyes have increased the light absorption effectiveness in comparison to malvidin. Because of this, the designed dyes may generate more electricity from sunlight.

Open circuit voltage: The open-circuit voltage (V_{OC}) of a DSSC is proportional to the potential energy gap between the redox potential of the electrolyte and the quasi-Fermi level of electron in the TiO_2 conduction band [23]. The Fermi level is defined by the potential of the conduction band (E_{CB}) and the electron density in the TiO_2. However, eqn. 4 can be used to calculate the (V_{OC}) of the DSSCs system based on the electron injection from the dye's LUMO level to the conduction band of TiO_2 [23]. The calculated (V_{OC}) values of the investigated dyes are listed in Table-4.

$$V_{oc} = E_{LUMO} - E_{cb} \quad (4)$$

Since V_{oc} is directly proportional to the power conversion efficiency of the solar cell. The maximum open circuit voltage was calculated for Ma5 dye molecule, which has a value of 0.1858 eV in DMF solvent phase and can be considered the most efficient DSSC sensitizer.

Electron coupling constant: Using the extended Mulliken-Hush (GMH) formalism, V_{RP} for a photo-induced charge transfer can be evaluated [13], where V_{RP} is the electronic coupling term and can be evaluated as follows [24]:

$$V_{RP} = \frac{\Delta E_{RP}}{2} \quad (5)$$

The injection driving force can be expressed within Koopman's approximation as:

$$\Delta E_{RP} = \left[E^{dye}_{LUMO} + 2E^{dye}_{HOMO}\right] - \left[E^{dye}_{LUMO} + E^{dye}_{HOMO} + E^{TiO_2}_{CBO}\right] \quad (6)$$

where $E^{TiO_2}_{CBO}$ is the conduction band edge. It is challenging to measure accurately $E^{TiO_2}_{CBO}$ because it is highly sensitive to the operating conditions. Thus, we have used $E^{TiO_2}_{CBO}$ = –4.0 eV [25], which corresponds to experimental conditions in which the semiconductor is immersed in aqueous redox electrolytes with a constant pH of 7.0, whereas the HOMO energy is related to the potential of the first oxidation *i.e.* ($E^{dye}_{HOMO} = E^{dye}_{OX}$).

$$\Delta E_{RP} = \left[E^{dye}_{OX} + E^{TiO_2}_{OX}\right] \quad (7)$$

In other words, a better sensitizer would have a greater V_{RP} since a larger V_{RP} leads to a higher rate constant [13]. Strong electrical interaction with the TiO_2 surface is promoted by the presence of NO_2 anchoring group and the cyano group of the LUMO.

Conclusion

For dye-sensitized solar cells, six novel organic D-π-A systems were designed by altering the moelcular structure of of malvidin. All of these dyes have been studied with TD-DFT calculations to determine their optimum properties. Both gas and liquid phases were studied to learn more about the opto electronic, electrochemical, and photovoltaic properties of the material. All of the designed sensitizers have HOMO and LUMO energy levels which are well-matched to the redox pair and the TiO_2 conduction band. The insertion of an electron source and acceptor caused a significant red shift in the value of λ^{max} for all six of the newly designed dyes, Ma1–Ma6. When compared to malvidin, both the light harvesting efficiency (LHE) and the free electron injection (ΔG^{inject}) were enhanced. This study demonstrated that improving electron injection and light harvesting efficiency can be achieved by adding an electron source and acceptor to a π-bridge. As a result of present studies, it is suggested that the novel designed dyes had potential as DSSC materials.

TABLE-4
OPEN-CIRCUIT VOLTAGE (V_{oc}) IN eV AND ELECTRON COUPLING CONSTANTS ($|V_{RP}|$) OF MALVIDIN BASED DYES

Dye	Gas phase		DMF		DCM	
	V_{oc}	$\|V_{RP}\|$	V_{oc}	$\|V_{RP}\|$	V_{oc}	$\|V_{RP}\|$
Malvidin	-2.5720	2.6029	0.4272	1.2418	0.1537	1.3602
Ma1	-2.6227	1.7568	0.1167	0.3942	-0.1418	0.5219
Ma2	-2.7092	1.8094	0.0522	0.4325	-0.2085	0.5627
Ma3	-2.5977	1.7338	0.0225	0.4325	-0.2303	0.5580
Ma4	-2.506	1.8175	0.1782	0.4819	-0.0822	0.6112
Ma5	-2.3735	1.7537	0.1858	0.4793	-0.0598	0.6011
Ma6	-2.3979	1.7666	-0.0852	0.6134	-0.0852	0.6139

CONFLICT OF INTEREST

The authors declare that there is no conflict of interests regarding the publication of this article.

REFERENCES

1. I.N. Obotowo, I.B. Obot and U.J. Ekpe, *J. Mol. Struct.*, **1122**, 87 (2016); https://doi.org/10.1016/j.molstruc.2016.05.080
2. E.C. Prima, B. Yuliarto, V. Suendo and Suyatman, *J. Mater. Sci. Mater. Electron.*, **25**, 4603 (2014); https://doi.org/10.1007/s10854-014-2210-x
3. B.B. Ma, R. Gao, L.D. Wang, Y.F. Zhu, Y.T. Shi, Y. Geng, H.P. Dong and Y. Qiu, *Sci. China Chem.*, **53**, 1669 (2010); https://doi.org/10.1007/s11426-010-4042-8
4. C.G. Garcia, A.S. Polo and N.Y. Murakami Iha, *J. Photochem. Photobiol. Chem.*, **160**, 87 (2003); https://doi.org/10.1016/S1010-6030(03)00225-9
5. M. Gratzel, *J. Photochem. Photobiol.*, **4**, 145 (2003); https://doi.org/10.1016/S1389-5567(03)00026-1
6. M.R. Narayan, *Renew. Sustain. Energy Rev.*, **16**, 208 (2012); https://doi.org/10.1016/j.rser.2011.07.148
7. S. El Mzioui, S.M. Bouzzine, I. Sidir, M. Bouachrine, M.N. Bennani, M. Bourass and M. Hamidi, *J. Mol. Model.*, **25**, 92 (2019); https://doi.org/10.1007/s00894-019-3963-1
8. B. Kim, K. Chung and J. Kim, *Chem. Eur. J.*, **19**, 5220 (2013); https://doi.org/10.1002/chem.201204343
9. A. Hagfeldt, G. Boschloo, L. Sun, L. Kloo and H. Pettersson, *Chem. Rev.*, **110**, 6595 (2010); https://doi.org/10.1021/cr900356p
10. I. Konczak and W. Zhang, *J. Biomed. Biotechnol.*, **2004**, 239 (2004); https://doi.org/10.1155/S1110724304407013
11. H.B. Singh and K.A. Bharati, Handbook of Natural Dyes and Pigments, Woodhead Publishing India Pvt. Ltd.: New Delhi, India, pp. 4-8 (2014).
12. K. Galappaththi, A. Lim, P. Ekanayake and M.I. Petra, *Int. J. Photoenergy*, **2017**, 8564293 (2017); https://doi.org/10.1155/2017/8564293
13. J.M. Juma, S.A.H. Vuai and N.S. Babu, *Int. J. Photoenergy*, **2019**, 4616198 (2019); https://doi.org/10.1155/2019/4616198
14. M.I. Abdullah, M.R.S.A. Janjua, A. Mahmood, S. Ali and M. Ali, *Bull. Korean Chem. Soc.*, **34**, 2093 (2013); https://doi.org/10.5012/bkcs.2013.34.7.2093
15. X. Xie, Z. Liu, W. Li, F. Bai, E. Lee and H. Zhang, *Chem. Phys. Lett.*, **719**, 39 (2019); https://doi.org/10.1016/j.cplett.2019.01.047
16. F. Santoro, A. Lami, R. Improta, J. Bloino and V. Barone, *J. Chem. Phys.*, **128**, 224311 (2008); https://doi.org/10.1063/1.2929846
17. S. Mathew, A. Yella, P. Gao, R. Humphry-Baker, B.F.E. Curchod, N. Ashari-Astani, I. Tavernelli, U. Rothlisberger, M.K. Nazeeruddin and M. Grätzel, *Nat. Chem.*, **6**, 242 (2014); https://doi.org/10.1038/nchem.1861
18. S. Elkhattabi, M. Hachi, A. Fitri, A.T. Benjelloun, M. Benzakour, M. Mcharfi and M. Bouachrine, *J. Mol. Model.*, **25**, 9 (2019); https://doi.org/10.1007/s00894-018-3888-0
19. M. Bourass, A.T. Benjelloun and M. Benzakour, *J. Mater. Environ. Sci.*, **7**, 700 (2016).
20. P. Ekanayake, M.R.R. Kooh, N.T.R.N. Kumara, A. Lim, M.I. Petra, N.Y. Voo and C.M. Lim, *Chem. Phys. Lett.*, **585**, 121 (2013); https://doi.org/10.1016/j.cplett.2013.08.094
21. M. Cossi and V. Barone, *J. Chem. Phys.*, **115**, 4708 (2001); https://doi.org/10.1063/1.1394921
22. M. Megala and B.J.M. Rajkumar, *J. Comput. Electron.*, **18**, 1128 (2016); https://doi.org/10.1007/s10825-019-01398-0
23. H. Roohi and N. Mohtamadifar, *RSC Adv.*, **12**, 11557 (2022); https://doi.org/10.1039/D2RA00906D
24. C.P. Hsu, *Acc. Chem. Res.*, **42**, 509 (2009); https://doi.org/10.1021/ar800153f
25. R.A. Marcus, *Rev. Mod. Phys.*, **65**, 599 (1993); https://doi.org/10.1103/RevModPhys.65.599